Alfven wave excitation and single-pass ion cyclotron heating in a fast-flowing plasma

doi: 10.1063/1.2178774

Alfvén wave excitation and single-pass ion cyclotron heating in a fast-flowing plasma[a)]

Akira Ando,[b)] Masaaki Inutake, Motoi Hatanaka, Kunihiko Hattori, Hiroyuki Tobari, and Tsuyoshi Yagai
Department of Electrical Engineering, Graduate School of Engineering, Tohoku University, Aoba-yama 05, Sendai 980-8579, Japan

(Received 20 October 2005; accepted 17 November 2005; published online 15 May 2006)

Alfvén wave excitation and ion heating experiments were performed in a fast flowing plasma. When rf waves in the ion cyclotron range of frequency were excited by right- and left-handed helically wound antennas, shear and compressional Alfvén waves with azimuthal mode number $m=-1$ and $m=+1$, respectively were excited. The dispersion relations of the propagating waves were obtained experimentally and compared with the theoretical ones, including the Doppler effect of the plasma flow. Strong ion heating was observed in the fast-flowing plasma when rf waves were launched by the right-handed helically wound antenna in a magnetic beach configuration. The plasma thermal energy $W_\perp$ and the ion temperature T_i drastically increased during the rf pulse. This large increase was observed under lower-density conditions, where the ratio of the ion cyclotron frequency to the ion-ion collision frequency becomes high. The resonance magnetic field was affected by the Doppler shift due to the fast-flowing plasma. © *2006 American Institute of Physics*.
[DOI: 10.1063/1.2178774]

I. INTRODUCTION

Recently, plasma flow has been recognized to play an important role in the behavior of space and fusion plasmas, such as the violent activities near the solar surface and the jet formation observed in active galactic nuclei.[1] The effect of high-speed plasma flow on the stability and transport of plasmas is a current topic in the field of fusion plasmas.[2] Intensive research to develop a fast-flowing plasma source with a high particle flux and a high heat flux is required for basic plasma physics as well as various industrial and space applications.

Electric propulsion systems utilize plasma as the exhaust matter and are one of the key elements of future space exploration projects.[3,4] The development of a high-power density plasma thruster with a higher specific impulse and a larger thrust is needed for manned interplanetary space thrusters. One feature of advanced space propulsion systems is their ability to vary the specific impulse by modulating propellant utilization and thrust performance. The ability to control the ratio of the specific impulse to the thrust at constant power will allow for optimum interplanetary trajectories, and will result in shorter trip durations than with fixed specific impulse systems.

One of the key technologies of the Variable Specific Impulse Magnetoplasma Rocket (VASIMR) project underway at NASA, is to control the ratio of the specific impulse to the thrust at constant power.[5,6] The rocket provides a helicon plasma source and a combined system of ion cyclotron heating and a diverging magnetic nozzle, where a flowing plasma is heated by ion cyclotron range of frequency (ICRF) heating and the plasma thermal energy is converted to a flow energy in the magnetic nozzle. This means that the magnetic nozzle effect and ICRF heating in fast-flowing plasma are two key issues for the development of an advanced space thruster.

Plasma acceleration in a divergent magnetic nozzle has been successfully demonstrated in a HITOP device using a magneto-plasma-dynamic arcjet (MPDA). The MPDA is one of the representative space thruster devices and is also utilized as a source of supersonic plasma flow.[7] The plasma produced in the MPDA is accelerated by the Lorentz force $J_r \times B_\theta$, where J_r is the radial component of the discharge current and B_θ is the azimuthal component of the self-induced magnetic field. The ion acoustic Mach number M_i of the exhausted plasma, which is defined as the ratio of the plasma flow velocity to the ion acoustic velocity, has been observed to be nearly unity. In an externally applied divergent magnetic nozzle configuration, a supersonic plasma flow with M_i of up to 3 has been obtained in the far downstream region of the MPDA, where no $J_r \times B_\theta$ acceleration is exerted.[8] It has also been demonstrated that the subsonic plasma flow exhausted from the MPDA can be converted into a supersonic one (where M_i exceeds unity) using a Laval-type magnetic nozzle attached in front of the MPDA muzzle.[9,10]

However, an efficient method of heating ions of a flowing plasma using rf waves is crucial for realizing an advanced thruster. Although ion heating in magnetically confined plasma has been precisely investigated both theoretically and experimentally in many researches, few attempts at wave excitation and direct ion heating in fast-flowing plasmas using rf waves have been carried out. Heating the ions in a fast flowing plasma might be difficult partly because the short transit time of a single passage of ions

[a)]Paper R12 6, Bull. Am. Phys. Soc. **50**, 309 (2005).
[b)]Invited speaker. Electronic mail: akira@ecei.tohoku.ac.jp

through the heating region, and partly because of the modification of the ion cyclotron resonance due to the Doppler shift.

The Alfvén wave is a typical low-frequency wave propagating along a magnetic field line. It is a hydromagnetic wave first predicted by Alfvén in the 1940s (Ref. 11) and has been found to play a crucial role in MHD phenomena in space plasmas. The shear Alfvén wave, which is a slow wave at $\omega/\omega_{ci}<1$, is a left-handed circularly polarized wave, and is also called an ion cyclotron wave near $\omega/\omega_{ci}=1$, because thermal ions resonate with the wave and are heated by absorbing the wave energy. It is important in both plasma physics and geophysics to investigate methods of Alfvén wave excitation and the characteristics of wave propagation in fast-flowing plasmas with the ion acoustic and the Alfvén Mach number, M_i and M_A, of nearly unity.

In laboratory plasmas, several excitation methods have been proposed to excite shear Alfvén waves in suitably dense and magnetized plasmas with the azimuthal mode number $m=-1$, excited inductively by a Nagoya-type-III antenna,[12,13] a helical antenna,[14,15] and other antenna structures.

We made the first attempt at the ion heating in a supersonic plasma flow produced by a MPDA using a pair of loop-type antennas to excite Alfvén waves.[16,17] In that study, we found that the plasma thermal energy measured by the diamagnetic loop coil increased when the rf waves were launched in the nonaxisymmetric azimuthal mode ($m=\pm 1$) in a beach-heating configuration. Recently, Chang Dìaz *et al.* reported ion heating in the plasma exhausted from a helicon plasma in a VX-10 device. They used a half-turn or a helical antenna and obtained evidence of ion heating; a change in the rf antenna loading resistance and in the ion energy distribution, as measured by retarding energy analyzers.[18,19] Theoretical research has also been performed for the VASIMR project.[20] Although helicon plasmas are feasible for continuous operation, the charge-exchange energy loss from the neutral gas deteriorates the heating efficiency in thin plasmas.

In the present experiments, a pulsed MPDA is installed on a HITOP device with a large volume and length in order to minimize the charge-exchange collision effect between energetic ions and neutral atoms. Preinjected neutral gas is reduced using a fast-acting-gas valve. The effect of the neutral gas produced on the end plate of the HITOP device by the surface recombination of the injected plasma is kept as low as possible. A helically wound antenna is used to excite the rf waves more efficiently and the ICRF heating experiments are performed in a fast-flowing plasma with an M_i value of nearly unity.

In Sec. III, the wave magnetic field measured by magnetic probes (B-dot probes) and the spatial structures of the wave magnetic field variation are presented. The dispersion relations of the wave propagating in a fast-flowing plasma are also discussed. In Sec. IV, ion heating experiments with single-pass interaction between the excited waves and the flowing plasma are presented. The effects of ion heating are evaluated using a diamagnetic coil and electrostatic energy analyzers. The dependence on the magnetic field, electron density, and ratio of the ion-ion collisional frequency to the ion cyclotron frequency is also discussed.

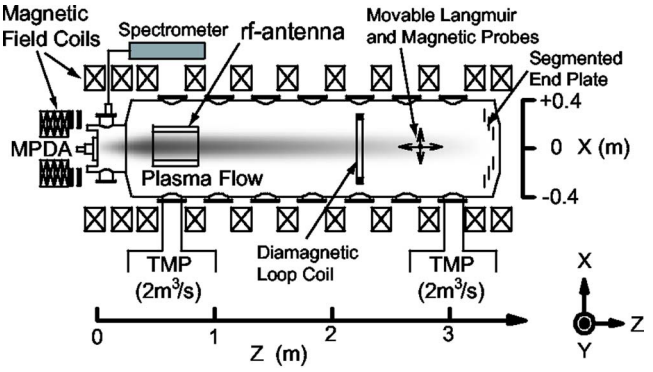

FIG. 1. A schematic of the HITOP device.

II. EXPERIMENTAL SETUP

A. HITOP device

The experiments were carried out in the HITOP device at Tohoku University. It consists of a large cylindrical vacuum chamber (diameter $D=0.8$ m, length $L=3.3$ m) with eleven main and six auxiliary magnetic coils, which generate a uniform magnetic field of up to 1 kG, as shown in Fig. 1. Various magnetic field configurations can be implemented by adjusting the external coil current.[8,16,21] A high power, quasisteady MPDA is installed at one end-port of the HITOP as a source of a fast-flowing plasma. It has a coaxial structure with tungsten rod cathode (10 mm in diameter) in the center and an annular molybdenum anode (30 mm in diameter). Discharge currents I_d of up to 10 kA are supplied by a pulse-forming network (PFN) system with a quasisteady duration of 1 ms. The current I_d is kept nearly constant during the discharge with a typical voltage of 200–300 V and can be controlled by varying the charging voltage of the capacitor banks of the PFN power supply. It can generate highly ionized, high density (more than 10^{20} m^{-3}), fast-flowing plasmas with M_i of up to 3 in an axial magnetic field B_z of up to 1 kG. The plasma density and the flow velocity increase almost linearly with I_d. Plasma densities below 10^{18} m^{-3}were obtained by inserting an electrically floated metal-mesh electrode downstream of the MPDA. The typical plasma flow velocity was 10–30 km/s with M_i of nearly unity. Helium or argon gas was used as the working gas in the experiments. The x, y, and z axes are shown in Fig. 1, where the origin of the z axis is set at the tip of the MPDA cathode.

The plasma flow characteristics are measured using several diagnostic tools installed on the HITOP device. The electron temperature T_e and density n_e profiles are measured using a movable Langmuir probe. The ion temperature T_i is measured using an electrostatic energy analyzer. The plasma thermal energy $W_\perp$ is measured at $Z=2.23$ m using a diamagnetic loop coil with a diameter of 400 mm. The spatial profiles of M_i and n_e along and across the field lines are measured using a movable Mach probe[22,23] and an array of 13-channel Mach probes set at 1.7 m downstream of the MPDA outlet on the HITOP. The time-varying magnetic

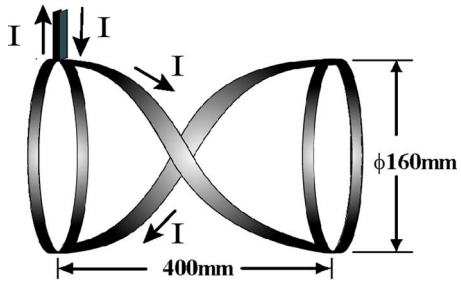

FIG. 2. A schematic of a right helical antenna.

fields associated with the excited waves in the plasma flow are measured directly using a movable magnetic probe array, consisting of 11 ch chip-sets of magnetic probes arrayed radially. Each probe has three sets of mutually perpendicular pick-up coils for measuring three components of the magnetic field variation ΔB_r, ΔB_θ, and ΔB_z. The probe signals (B dot signals) and the diamagnetic coil signal are transferred to differential amplifiers and integrators and are stored in digital data recorders.

B. Helical antenna and rf power source

We prepared two types of helically wound antennas to excite rf waves in the plasma. Figure 2 shows a schematic of a half-turn right-handed helically wound antenna 160 mm in diameter and 400 mm in length. There are two winding directions for the conductor. One is the right-handed helical winding, clockwise along the B_z field, and this type of antenna will be called a right helical antenna henceforth; the other will be called a left helical antenna. Our intention is to use the right and left helical antennas to excite rf waves downstream of the antenna, preferably with the azimuthal mode numbers $m=-1$ and $+1$, respectively.[14]

The electric field of the waves is expressed as follows:

$$E = E_0 \exp i(k_{//}z + m\theta - \omega t). \tag{1}$$

One of the antennas was set at $Z=0.6$ m downstream of the MPDA. The antenna current was supplied by inverter-type power sources operated in a pulsed mode, as shown in Fig. 3. We are able to change the oscillating frequency by controlling the external oscillator. One of the rf sources can excite oscillating currents with frequencies from 20 to 160 kHz in order to measure wave propagation in the plasmas. The other can excite rf power of up to 15 kW with frequencies from 100 to 400 kHz, and the rf power is used mainly for ion heating.

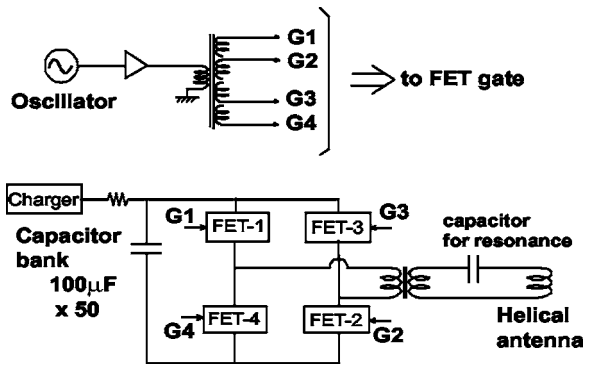

FIG. 3. An electric circuit diagram of the rf power supply.

III. ALFVÉN WAVE EXCITATION IN A FAST-FLOWING PLASMA

The Alfvén wave is a typical low-frequency wave propagating along a magnetic field line.[24] At frequencies below the ion cyclotron range of frequency $\omega_{ci}/2\pi$, $(\omega < \omega_{ci} \ll \omega_{ce}, \omega_{pe})$, the dispersion relation of the Alfvén wave propagating in a uniform plasma along the external magnetic field B is expressed as follows:

$$\omega^2 = k_{//}^2 V_A^2 \left(1 \pm \frac{\omega}{\omega_{ci}}\right), \tag{2}$$

where $k_{//}$ is the field-aligned component of the wave number k, and V_A is the Alfvén velocity. The Alfvén velocity is expressed as follows:

$$V_A = B/\sqrt{\mu_0 n_i m_i}, \tag{3}$$

where, μ_0 is the permeability, n_i is the ion density, and m_i is the ion mass. The notations + and − in Eq. (2) refer to a fast (compressional) wave and a slow (shear) wave, respectively.

In a plasma moving along a uniform magnetic field, the dispersion relation should be modified by taking into account the effect of the Doppler shift. This is done by replacing ω with $\omega - k_{//}U$, where U is the plasma flow velocity. Then the dispersion relation is expressed as follows:

$$(\omega - k_{//}U)^2 = k_{//}^2 V_A^2 \left(1 \pm \frac{(\omega - k_{//}U)}{\omega_{ci}}\right). \tag{4}$$

Now, we introduce the following normalized parameters: $\Omega_i = \omega/\omega_{ci}$, $K = k_{//}c/\omega_{pi}$ and the Alfvén Mach number $M_A = U/V_A$. By using the relation $\omega_{ci}/\omega_{pi} = c/V_A$, where c is the velocity of light, Eq. (4) can be expressed as follows:

$$(\Omega_i - KM_A)^2 = K^2[1 \pm (\Omega_i - KM_A)]. \tag{5}$$

Then, we obtain

$$\Omega_i = \frac{K}{2}\left(2M_A \pm K + \sqrt{K^2 + 4}\right). \tag{6}$$

Equation (6) is the dispersion relation of a compressional (+) and a shear (−) Alfvén wave in a flowing plasma with the Alfvén Mach number M_A.[25]

The right helical antenna tends to excite rf waves which propagate downstream and azimuthally in the counterclockwise direction with $m=-1$. This corresponds to a slow wave, a shear Alfvén wave, in the low-frequency region. The left helical antenna, on the other hand, tends to excite rf waves which propagate downstream and azimuthally in the clockwise direction with $m=+1$, which corresponds to a fast wave, a compressional Alfvén wave.[14]

In order to identify the propagating rf waves excited by the two types of antenna (right and left helical antennas), we measured the wave amplitudes and phase shifts using magnetic probes in a uniform magnetic field configuration. By changing the excitation frequency f_{rf}, the wavelength was

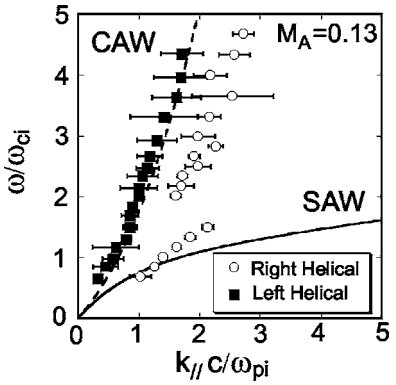

FIG. 4. The dispersion relations of the propagating wave in an argon plasma. rf waves are excited by the right (open circles) and left (closed squares) helical antennas. B=0.79 kG (uniform). The solid and dashed lines are the calculated dispersion relations of the shear ($m=-1$) and compressional ($m=+1$) Alfvén waves propagating downstream of the antenna in a uniform plasma, respectively, with the Alfvén Mach number M_A=0.13.

obtained from the phase difference between the two magnetic probe signals located in the downstream region, at Z=1.03 m and 1.43 m.

Figure 4 shows the dispersion relations observed under a uniform magnetic field of 0.79 kG, where the ion cyclotron resonance frequency ($f_{ci}=\omega_{ci}/2\pi$) is 30 kHz for argon plasma. The dispersion relations of the shear and compressional Alfvén waves are calculated using Eq. (5) and are shown in Fig. 4 with an Alfvén Mach number M_A of 0.13, which corresponds to the experimental condition.

The wave excited by the right helical antenna agrees well with the dispersion curve of the shear Alfvén wave at $\omega/\omega_{ci}<1.5$ and coincides well with that of the compressional wave at $\omega/\omega_{ci}>2$. The wave excited by the left helical antenna corresponds well to the dispersion curve of compressional wave for all frequency ranges.

Figure 5 shows the spatial structures of the time-varying magnetic field associated with the waves. The time evolutions of the field structure indicate the behavior of left- and right-handed, circular polarizations in the core region, which correspond to the azimuthally propagating modes with $m=-1$ and $m=+1$, excited by the right helical antenna under the conditions $\omega/\omega_{ci}=1$ (f_{rf}=30 kHz) and $\omega/\omega_{ci}=2.6$ (f_{rf}=80 kHz), respectively.

IV. ION HEATING THROUGH A SINGLE-PASS INTERACTION BETWEEN THE RF WAVES AND THE FLOWING PLASMA

Ion heating experiments were performed in a magnetic beach configuration in order to couple the excited rf waves with the flowing plasma. Figure 6 shows an axial profile of the magnetic field strength and the locations of the rf antenna and the diamagnetic coil. The upstream magnetic field B_U was kept constant and the downstream magnetic field B_D was varied to form a magnetic beach configuration as well as a uniform magnetic field. The right helical antenna was used to launch slow waves (ion cyclotron waves) at $\omega/\omega_{ci}<1$ and the waves propagated downward in the magnetic beach configuration, approaching $\omega/\omega_{ci}=1$.

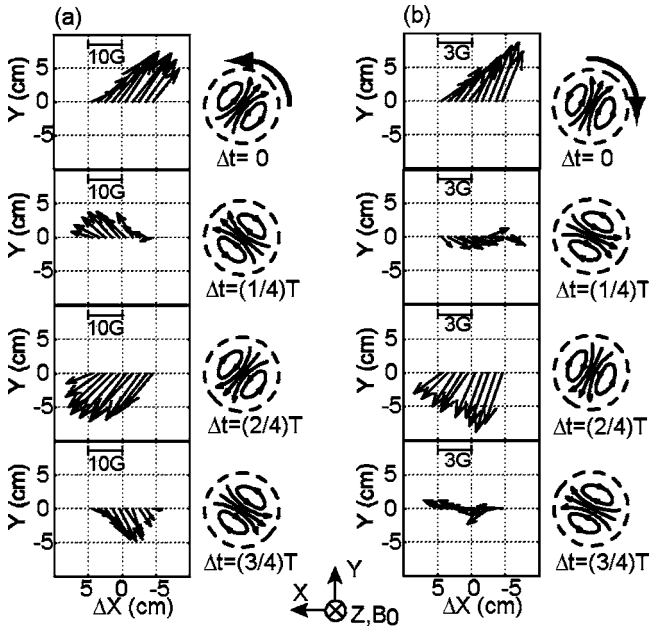

FIG. 5. The spatial structures of the time-varying magnetic field associated with the waves excited by the right helical antenna. (a) $\omega/\omega_{ci}=1$(f_{rf}=30 kHz) and (b) $\omega/\omega_{ci}=2.6$ (f_{rf}=80 kHz). Ar plasma. Uniform magnetic field of 0.79 kG.

Figure 7 shows the typical waveforms of the discharge current I_d and the observed diamagnetic coil signal $W_\perp$, which corresponds to the component of the plasma thermal energy perpendicular to the magnetic field. When the rf waves were excited, $W_\perp$ drastically increased as shown in the figure.

The ion temperature T_i was measured by electrostatic energy analyzers (EEA) set at the diamagnetic coil position of Z=2.23 m. The EEA consists of a metal plate with a small circular hole and three grids. Ions pass through the small hole and are reflected by a retarding voltage applied between the grids. By making the normal of the hole parallel and perpendicular to the plasma flow, we were able to obtain both components of the ion temperature, $T_{i//}$ and $T_{i\perp}$.

The perpendicular ion-temperature component $T_{i\perp}$ increased from 3.9 eV to nearly 40 eV at the rf output power P_{rf} of 15 kW. The increments of $T_{i\perp}$ and $W_\perp$ were almost linearly proportional to P_{rf} as shown in Fig. 8. The electron

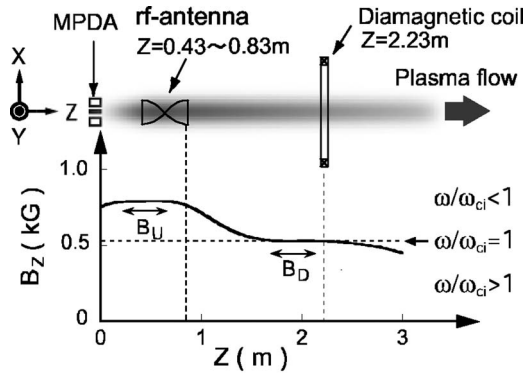

FIG. 6. The magnetic configuration and locations of the rf antennas and the diamagnetic coil.

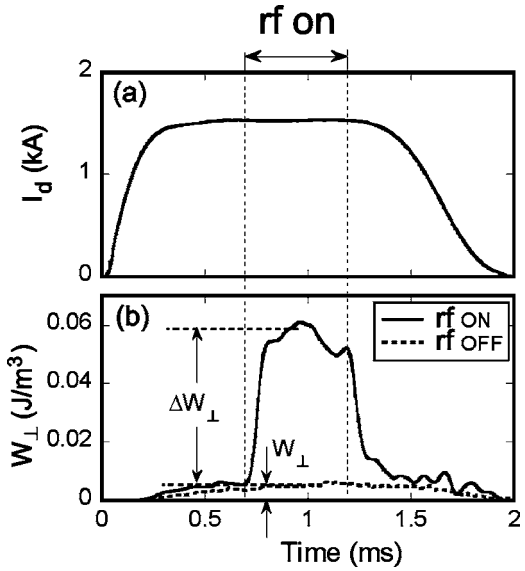

FIG. 7. The time evolutions of (a) the discharge current I_d and (b) the diamagnetic coil signal $W_\perp$. He plasma. B_U=1 kG and B_D=0.575 kG. f_{rf} =236 kHz.

density n_e and the electron temperature T_e were measured using a Langmuir probe just after the rf were turned off, in order to eliminate the oscillating field effect on the probe measurement. The electron density was $0.3-0.5\times10^{18}$ m^{-3} and it decreased slightly during the rf excitation, whereas the electron temperature nearly doubled. The increments of T_i and T_e were measured at different positions in the downstream region and are plotted in Fig. 9. Both temperatures increased, not in the region just downstream of the rf antenna but in the plateau region of the magnetic beach configuration. The larger increase in T_i than in T_e in the plateau region indicates the preferential heating of ions in the flowing plasma. The increment of $W_\perp$ was qualitatively consistent with those of T_i and T_e.

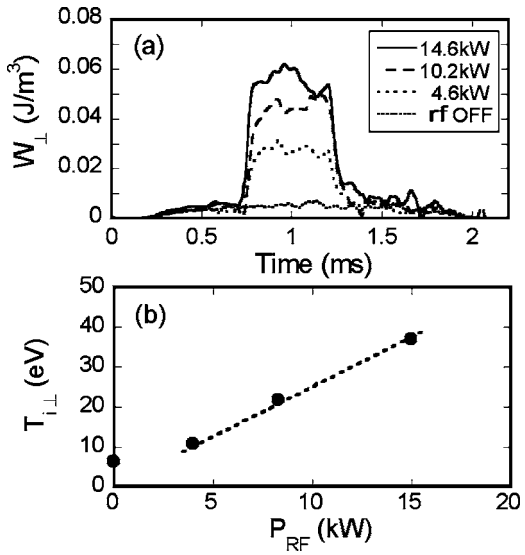

FIG. 8. (a) The time evolutions of $W_\perp$ for various rf powers. (b) The dependence of the ion temperature T_i as a function of the rf power. He plasma. f_{rf}=236 kHz.

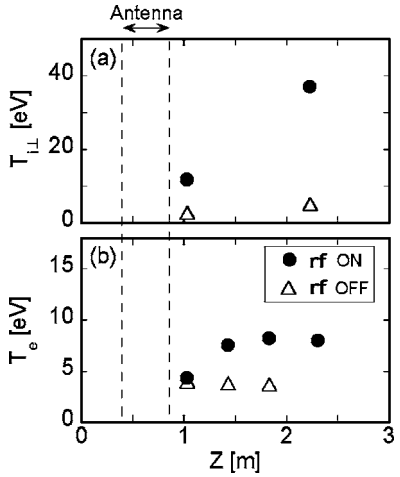

FIG. 9. The axial profiles of (a) T_i and (b) T_e with and without P_{rf}. He plasma. f_{rf}=236 kHz.

In order to clarify the ion cyclotron resonance heating, we varied the magnetic field B_D in the downstream region. Figure 10 shows the dependence of $\Delta W_\perp/W_\perp$ on the magnetic field B_D for three different rf frequencies. The magnetic field configuration was of the magnetic-beach-type with a constant B_U of 0.7 kG for f_{rf}=80 and 164 kHz, and of 1.0 kG for f_{rf}=238 kHz at the antenna position and a variable B_D at the diamagnetic coil position. The vertical solid lines in Fig. 10 indicate the B_D corresponding to ω/ω_{ci}=1 for each excited rf frequency. $\Delta W_\perp/W_\perp$ became large near the B_D at ω/ω_{ci}=1 for three different rf frequencies. It was also observed that the peak shifted slightly to a lower B_D than that corresponding to ω/ω_{ci}=1, i.e., ω/ω_{ci} was higher than 1. This shift was not caused by the diamagnetic effect, which would make the resonance field shift to a higher B_D, although the beta value in the present experiments was low. The shift is in good agreement with the value predicted by the Doppler effect of the fast plasma flow.

When the B_D field is lowered to less than the value at ω/ω_{ci}=1, the resonance position shifts to the steep diverging region upstream of the plateau region. In this case, as shown in Fig. 10 the heating efficiency becomes lower than with the resonance in the plateau region. This indicates that the pla-

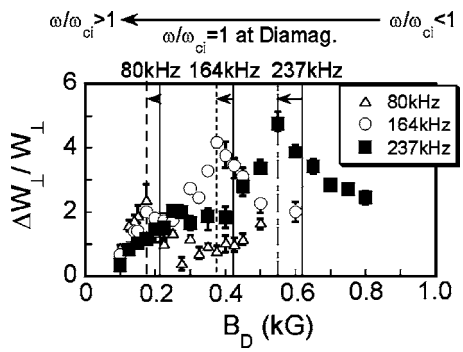

FIG. 10. The ratio of $\Delta W_\perp/W_\perp$ as a function of the downstream magnetic field B_D. He plasma. The solid lines correspond to ω/ω_{ci}=1 for the wave frequencies of f_{rf}=237 kHz (closed square), 164 kHz (open circle), 80 kHz (open triangle).

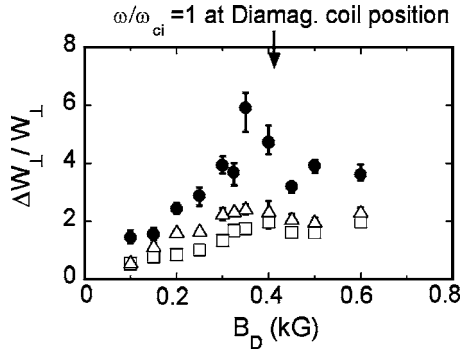

FIG. 11. The ratio of $\Delta W_\perp / W_\perp$ as a function of B_D. Helium plasma. B_U=0.7 kG. $f_{\rm rf}$=160 kHz. Closed squares: $f_{\rm rf}/\nu_{ii}$=8.4 ($n=0.52\times10^{18}$ m^{-3}), open triangles: $f_{\rm rf}/\nu_{ii}$=2.4($n=1.9\times10^{18}$ m^{-3}), open squares: $f_{\rm rf}/\nu_{ii}$=1.6($n=2.7\times10^{18}$ m^{-3}).

teau region with a gradual field variation is very important for the effective ion cyclotron damping of the excited waves in a magnetic beach configuration.

It was found that strong ion cyclotron heating occurred when the plasma density was lower than 10^{18} m^{-3}. Figure 11 shows dependence of the ratio $\Delta W_\perp / W_\perp$ on B_D for three different plasma densities. The magnetic field configuration was of the magnetic-beach-type with a constant B_U of 0.7 kG at the antenna position and a variable B_D at the diamagnetic coil position. As is shown in Fig. 11, there is a clear indication of the ion cyclotron resonance only at the plasma density of $n_e=0.5\times10^{18}$ m^{-3}. Under higher density conditions, the ion-ion collision frequency ν_{ii} becomes higher than the ion cyclotron frequency f_{ci} and the waves are damped not by cyclotron resonance but by collisional damping. Ions cannot gyrate in the Larmour motion between collisions, and therefore strong ion cyclotron heating does not occur. When the ratio $f_{\rm rf}/\nu_{ii}$ is low, $\Delta W_\perp / W_\perp$ does not show a large difference for different magnetic configurations.[26] Figure 12 shows the relations between ν_{ii} and n_i for helium gas and argon gas. The right-hand axis of the ordinate shows the magnetic field corresponding to the condition of $f_{ci}=\nu_{ii}$. The condition that $f_{\rm rf}/\nu_{ii}>1$ is satisfied in the region above the solid line.

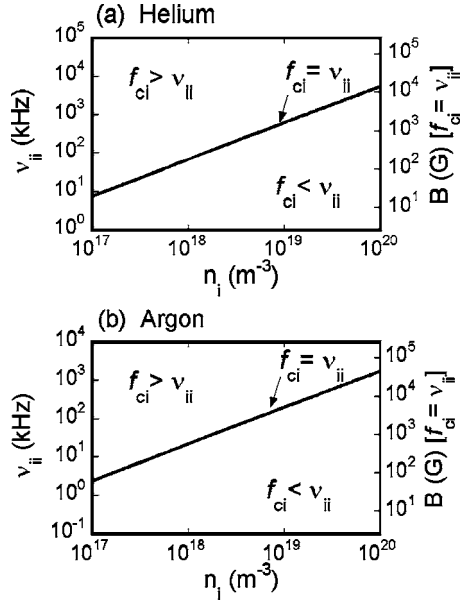

FIG. 12. The ion-ion collision frequency ν_{ii} as a function of the ion density n_i for (a) helium and (b) argon plasmas. T_i=4 eV is assumed. The right-hand axis of the ordinate corresponds to the magnetic field where $f_{ci}=\nu_{ii}$.

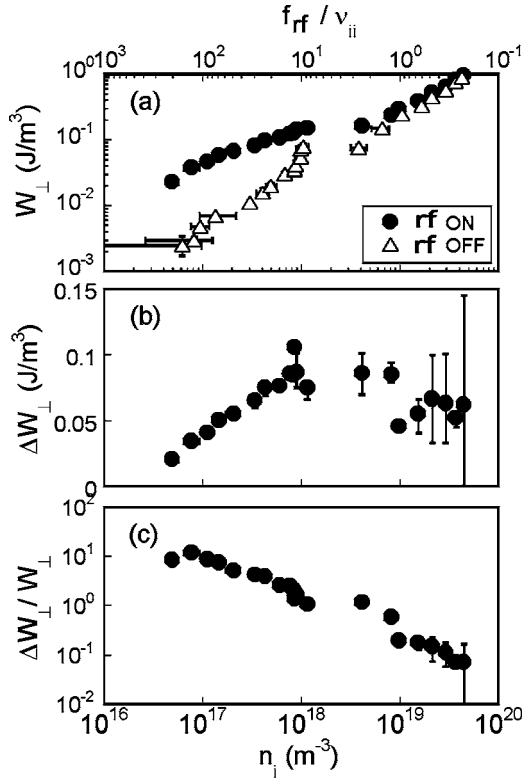

FIG. 13. The dependence of (a) $W_\perp$, (b) $\Delta W_\perp$, and (c) $\Delta W_\perp / W_\perp$ on n_i. He plasma. $P_{\rm rf}$=15 kW. $f_{\rm rf}$=236 kHz.

We varied the plasma density from 10^{17} to 10^{20} m^{-3} and measured the effect of the ion density on the ion heating. Figure 13 shows the observed variations in $W_\perp$, $\Delta W_\perp$, and $\Delta W_\perp / W_\perp$ for a wide range of n_i. A tenfold rise in $\Delta W_\perp / W_\perp$ was obtained for a low n_i around 10^{17} m^{-3}, where the ratio $f_{\rm rf}/\nu_{ii}$ is nearly 100. On the other hand, the increment of the thermal energy $\Delta W_\perp$ reached its maximum at the higher density of n_i ($=10^{18}-10^{19}$ m^{-3}). This is related to the variation of the antenna-plasma coupling. The length of the half-turn helical antenna used in the experiments was 0.4 m, which is suitable for exciting waves with a wavelength of 0.8 m. We measured the magnetic field intensity $|\tilde{B}|$ of the excited wave using a magnetic probe placed at Z=1.04 m. The propagating wavelength $\lambda_{//}$ was evaluated based on the phase difference between the two magnetic probe signals set at Z =1.04 m and 1.44 m. In Fig. 14 $|\tilde{B}|$ and $\lambda_{//}$ are plotted as a function of n_i. The upper axis of the abscissas shows the calculated values of $\lambda_{//}$ for each ion density using the following simple equation valid for low frequencies,

$$\lambda_{//} = V_A/f_{ci} = \frac{2\pi}{e}\sqrt{\frac{m_i}{\mu_0 n_i}}. \tag{7}$$

When the excited wavelength is well matched with the antenna wavelength at higher ion densities, the excited wave

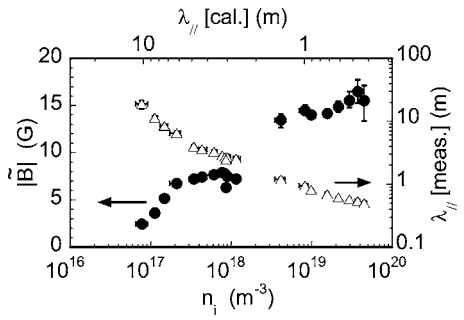

FIG. 14. The magnetic field amplitude $|\tilde{B}|$ and the wavelength $\lambda_{//}$ of the propagating wave as a function of n_i. He plasma. $P_{\mathrm{rf}}=15$ kW. $f_{\mathrm{rf}}=236$ kHz.

amplitude is large. We were able to optimize the length and diameter of the antenna for more efficient ion heating.

Although cyclotron damping is not effective at $f_{\mathrm{rf}}/\nu_{ii}<1$ in higher-density plasma, the increment of the plasma thermal energy is still observed. This collisional damping mechanism also plays an important role in a high-density plasma under lower magnetic fields. This heating scenario seems to be feasible in space propulsion applications because it is possible to eliminate large superconducting magnets to produce a strong magnetic field.

The heated ion energy should be converted to flow energy by passing it through a divergent magnetic nozzle. The experimental verification of the energy conversion will be presented in a separate paper.

V. CONCLUSIONS

Alfvén wave excitation and ion heating in a fast-flowing plasma for use in an advanced plasma thruster were investigated experimentally. Waves near the ion cyclotron frequency in the nonaxisymmetric $(m=\pm 1)$ mode were launched by right- and left-handed, helically wound antennas. Both the wave amplitude and phase shift were measured, and the dispersion relations of the propagating waves were obtained. The right helical antenna excites a shear Alfvén wave and the left helical one excites a compressional wave at $\omega/\omega_{ci}<1.5$.

The plasma thermal energy $W_{\perp}$ and the ion temperature T_i, as measured using the electrostatic energy analyzer, were observed to increase drastically when a slow wave was excited in a magnetic beach configuration. T_i increased from 4 to 40 eV at the rf output power P_{rf} of 15 kW. The magnetic field dependence of the measured $W_{\perp}$ clearly indicated the ion cyclotron resonance of thermal ions. The value of the resonance magnetic field was affected by the Doppler shift due to the fast-flowing plasma. This large increment of $W_{\perp}$ was observed at low densities, at which the ratio of the ion cyclotron frequency to the ion-ion collision frequency becomes large.

ACKNOWLEDGMENTS

This work was supported in part by a Grant-in-Aid for Scientific Research from the Japan Society for the Promotion of Science. Part of this work was carried out under the general coordinate researches of the National Institute of Fusion Science and the cooperative research project program of the Research Institute of Electrical Communication, Tohoku University.

[1] D. L. Meier, S. Koide, and Y. Uchida, Science **291**, 84 (2001).
[2] S. M. Mahajan and Z. Yoshida, Phys. Rev. Lett. **81**, 4863 (1998).
[3] R. G. Jahn, in *Physics of Electric Propulsion*, edited by H. S. Seifert (McGraw-Hill, New York, 1968).
[4] R. H. Frisbee, J. Propul. Power **19**, 1129 (2003).
[5] F. R. ChangDìaz, J. P. Squire, R. D. Bengston, B. N. Breizman, F. W. Baity, and M. D. Carter, in Proceedings of the 36th AIAA/ASME/SAE/ASEE Joint Propulsion Conference, Huntsville (2000) (The American Institute of Aeronautics and Astronautics, 2000), AIAA-2000-3756.
[6] F. R. ChangDìaz, Sci. Am. **283**, 90 (2000); Fusion Sci. Technol. **43**, 3 (2003).
[7] K. Kuriki and M. Inutake, Phys. Fluids **5**, 92 (1974).
[8] M. Inutake, A. Ando, K. Hattori, H. Tobari, and T. Yagai, J. Plasma Fusion Res. **78**, 1352 (2002).
[9] M. Inutake, Y. Hosokawa, R. Sato, A. Ando, H. Tobari, and K. Hattori, Fusion Sci. Technol. **47**, 191 (2005).
[10] H. Tobari, M. Inutake, A. Ando, and K. Hattori, J. Plasma Fusion Res. **80**, 651 (2004).
[11] H. Alfvén, Nature (London) **150**, 405 (1942).
[12] T. Watari, T. Hatori, R. Kumazawa *et al.*, Phys. Fluids **21**, 2076 (1978).
[13] Y. Ohsawa, M. Inutake, T. Tajima, T. Hatori, and T. Kamimura, Phys. Rev. Lett. **43**, 1246 (1979).
[14] Y. Amagishi, M. Inutake, T. Akitsu, and A. Tsushima, Jpn. J. Appl. Phys. **20**, 2171 (1981).
[15] W. Gekelman, S. Vincena, N. Palmer, P. Pribyl, D. Leneman, C. Mitchell, and J. Maggs, Plasma Phys. Controlled Fusion **42**, B15 (2000).
[16] M. Inutake, A. Ando, K. Hattori, T. Yagai, H. Tobari, R. Kumagai, H. Miyazaki, and S. Fujimura, Fusion Sci. Technol. **43**, 118 (2003).
[17] A. Ando, R. Kumagai, S. Fujimura, T. Yagai, K. Hattori, and M. Inutake, *AIP Conference Proceedings*, edited by Ian S. Falconer (American Physical Society, New York, 2002), Vol. 669, p. 298.
[18] J. P. Squire, F. R. ChangDìaz, T. W. Glover *et al.*, Fusion Sci. Technol. **43**, 111 (2003).
[19] F. R. ChangDìaz, J. P. Squire, T. W. Glover *et al.*, in Proceedings of the 42nd Aerospace Sciences Meeting and Exhibit, Reno (2004) (The American Institute of Aeronautics and Astronautics, 2004), AIAA-2004-0149.
[20] A. V. Arefiev and B. N. Breizman, Phys. Plasmas **11**, 2942 (2004).
[21] A. Ando, M. Ashino, Y. Sagi, M. Inutake, K. Hattori, M. Yoshinuma, A. Imasaki, H. Tobari, and T. Yagai, J. Plasma Fusion Res. **4**, 373 (2001).
[22] A. Ando, T. S. Watanabe, T. K. Watanabe, H. Tobari, K. Hattori, and M. Inutake, J. Plasma Fusion Res. **81**, 451 (2005).
[23] A. Ando, T. K. Watanabe, T. Makita, H. Tobari, K. Hattori, and M. Inutake, "Mach probe measurements in unmagnetized plasmas with subsonic and supersonic flow," Contrib. Plasma Phys. (to be published).
[24] R. C. Cross, in *An Introduction to Alfvén Wave*, The Adam Hilger Series on Plasma Physics (IOP, New York, 1989).
[25] T. Yagai, R. Kumagai, Y. Hosokawa, K. Hattori, A. Ando, and M. Inutake, *AIP Conference Proceedings*, edited by Ian S. Falconer (American Physical Society, New York, 2002), Vol. 669, p. 137.
[26] A. Ando, T. S. Watanabe, T. K. Watanabe, R. Sato, K. Harata, H. Tobari, K. Hattori, and M. Inutake, "Ion heating experiment by a helical antenna in a fast-flowing plasma," Thin Solid Films (to be published).